<Title of Publication> <*Edited by…*>
Materials Science and Technology (MS&T), 2006

Thermo-metallurgical model of the cooling table for a flat product hot rolling mill

G. Gomez[(1)], J. Schicht[(1)], T. Perez[(1)], M. Goldschmit[(1)], A. Vigliocco[(2)]

[1]Center for Industrial Research, Tenaris, Dr. Simini 250, B2804MHA Campana, Argentina
[2]TerniumSiderar, Av. Gral. Savio S/n, 2900 San Nicolas, Argentina

Keywords: Thermo-metallurgical model, hot rolling product, cooling table

Abstract

A coupled model that predicts the thermal and microstructural evolution of plain carbon steels in the cooling table of a flat product hot rolling mill was developed.
A finite element model is used to calculate the heat transfer of the sheet during the cooling table. The thermal properties of the steel such as the thermal conductivity, the specific heat and the reaction heat due to the metallurgical transformation are calculated by the metallurgical model. The non-linear equations are solved using a Newton-Raphson scheme and line search.
The metallurgical model describes the austenite decomposition into ferrite, perlite and bainite. It uses classical nucleation and early growth theories to calculate the beginning of the ferritic reaction, and Avrami-type equations to evaluate the transformation progress.
The coupled model was tested against mill measurements of coiling temperatures, and good results were obtained.

1. Introduction

Hot strip final microstructure and mechanical properties depend on the steel chemical composition and the applied thermo mechanical treatment. Rolling parameters, cooling conditions in both, the runout table and the coil, determine the resultant microstructure for each particular chemical composition. As customers are demanding higher requirements in terms of mechanical properties and quality, it is of paramount importance to have a tool to design steel chemistry and process conditions.
The thermo-metallurgical model for the cooling table presented in this paper was designed within the framework of a more comprehensive project aimed to develop a model for predicting mechanical properties of as rolled steels (including variations inside the coil). The cooling table model, called Thermet, was based on previously published works on thermal evolution of plates during water jet impingement [1-6], as well as some existing non-coupled [3; 4; 7-11] and coupled [12-14] thermo-metallurgical models.
Thermet consists of a metallurgical model, described in Section 2, coupled to a thermal finite element model, described in Section 3. The metallurgical model calculates the austenite decomposition into ferrite, perlite and/or bainite. It also evaluates the enthalpy and specific heat of the system needed for the coupling with the thermal model. The algorithm of Thermet is shown in Figure 1.

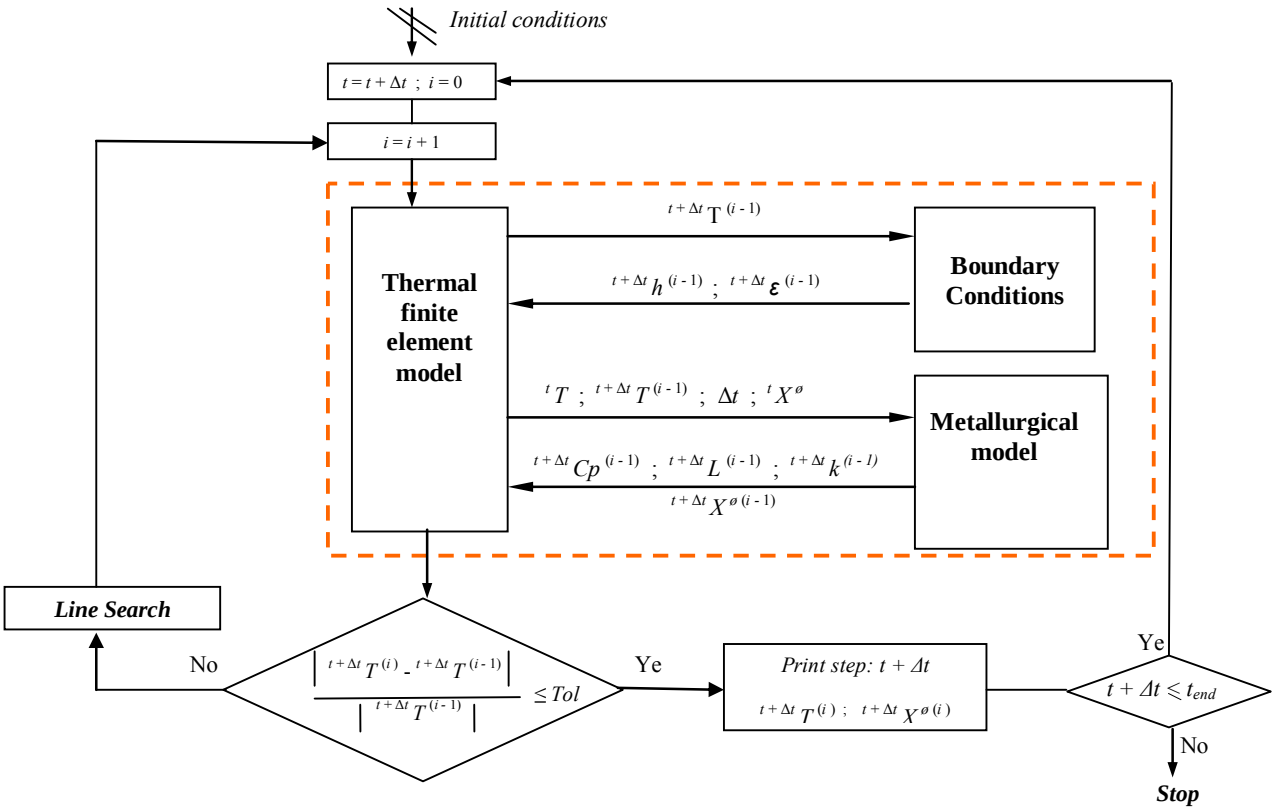

Figure 1 –Flux diagram for the thermo metallurgical coupling model.
t: time T : temperature h: heat transfer coefficient Cp: specific heat k: thermal conductivity
i: iteration X^{Φ}: phase fraction ε: emithance L : release heat Tol: tolerance

The description of the cooling table, and the boundary conditions for the numerical model applied to TerniumSiderar hot strip mill are presented in Section 4. The model was validated with measurements performed at TerniumSiderar hot rolling mill, as described in Section 5.

2. Metallurgical model for phase transformation

The metallurgical model for phase transformation during cooling from the austenitic range was described in detail elsewhere [15]. Only a brief description of this model is presented here. For simplicity the austenite decomposition was divided in two stages: i) the transformation start, which includes the first 1% of the reaction (in volume fraction), and ii) the reaction progress, which includes the rest of the transformation. For the range of steel chemistries and processing conditions considered in this work, the transformation start comprises the proeutectoid ferrite nucleation and its early growth. The transformation progress includes the remaining ferritic reaction, as well as the other possible reactions: formation of perlite and/or bainite.
The start of the proeutectoid ferrite reaction was evaluated using classical nucleation and growth theories in combination with the extended volume formalism [16]. Within this approach volume fraction of ferrite is given by:

$$\chi_F(t) = 1 - \exp\left(\int_0^t J(\tau)\, V(t,\tau)\, d\tau \right) \qquad (1)$$

where $J(\tau)$ is the nucleation rate by unit volume at time τ and $V(t,\tau)$ is the volume at time t of the ferrite grains formed at τ. To integrate Eq. (1), the origin of time (t = 0) was set when the material temperature drop below the equilibrium Ae3 line. The phase diagram was constructed using the paraequilibrium model [17] and the thermodynamical data presented by Miettinen [18].
The coherent pillbox model for ferrite nucleation at austenite grain boundaries [19] together with the carbon diffusion coefficient of Agren [20] and the interfacial energies reported by Tanaka *et al*. [21] were used to evaluate the nucleation rate. The number of nucleation sites per unit volume was taken proportional to the austenite grain boundary area per unit volume: $N = N_0 / d_\gamma$ where d_γ is the austenitic grain size. Since no intragranular nucleated ferrite was experimentally observed in the ranges of steel chemistries and cooling rates studied, this type of nucleation was not considered in the model.

Within the paraequilibrium approach, the growth of the ferrite nucleus was considered to be controlled by diffusion of carbon in austenite, and was evaluated using:

$$\frac{d\,r}{dt} = F(\Omega)\,\frac{D_C^\gamma}{r} \qquad \Omega = \frac{c^{\gamma\alpha} - c^{\gamma}}{c^{\gamma\alpha} - c^{\alpha\gamma}} \qquad (2)$$

where r is the radius of the ferrite grain; $c^{\gamma\alpha}$, $c^{\alpha\gamma}$ and c^{γ} are the carbon concentrations in austenite in equilibrium with ferrite, in ferrite in equilibrium with austenite, and in austenite far from the growing nucleus, respectively. The function F depends on the super-saturation ratio Ω, and was evaluated using the stationary-interface approximation for $|\Omega| < 0.7$ and the linearized-gradient approximation for $|\Omega| \geq 0.7$ [22].
The physical model for nucleation and early growth of ferrite has only one parameter to be empirically adjusted, i.e. N_0. For all the steels studied the same N_0 value was used, which was fitted by comparison between model predictions and experimental results for C-Mn steels [15].
The progress of the proeutectoid ferrite, perlite and bainite reactions was described using Avrami type equations:

$$\chi^{\phi} / \chi_{eq} = 1 - \exp\left[-\Psi \cdot t^{n}\right] \qquad (3)$$

where χ^{ϕ} is the volume fraction occupied by phase ϕ at time t (ϕ: ferrite, perlite or bainite), and χ_{eq} is the thermodynamic equilibrium fraction for proeutectoid ferrite, or the maximum available volume fraction in the case of perlite and bainite. The following functional form of ψ was adopted:

$$\Psi = \frac{A(T - T_0)^p \exp(-Q/RT)}{F(d_\gamma, \text{chemistry})} \qquad F(d_\gamma, \text{chemistry}) = \exp(B_0 + \sum B_j\, C_j) / d_\gamma^{\,m} \qquad (4)$$

where d_γ is the previous austenitic grain size, T_0 is the start temperature for each reaction, and C_j is the concentration in weight percent of the element j in solid solution in austenite (j: C, Mn, Si, Nb, V). The start temperature for the proeutectoid ferrite reaction was calculated from the nucleation and early growth model described in the previous section. The T_0 value for the perlitic reaction was estimated with the aid of the phase diagram, as shown by Senuma *et al.* [23]. The beginning of the bainitic transformation was calculated using an empirical expression (3) that takes the chemical composition of the steel, the cooling rate, and the previous austenitic grain size into account.
The empirical parameters that appear in eq. (4) were fitted for each possible reaction (ferrite, perlite or bainite) using data obtained from bibliography and from dilatometric tests performed on plain carbon and microalloyed steels (Table I). The dilatometric tests were conducted on a thermo-mechanical

simulator Gleeble 3500 for cooling rates in the range between 5 and 50°C/sec. The austenization conditions were chosen to get approximately the same autenitic grain size prior to transformation than during industrial operation. A detailed description of the experimental procedure was presented in reference [15].

Table I. Chemical compositions of the steels used to fit the phase transformation model

Steel	C [wt%]	Mn [wt%]	Si [wt%]	V [wt%]	Nb [wt%]	Ti [wt%]
CMn1	0.15	0.58	0.16	-	-	-
CMn2	0.15	1.15	0.15	-	-	-
V	0.15	1.09	0.17	0.046	-	-
Nb-Ti	0.13	1.43	0.14	-	0.036	0.016
V-Nb-Ti	0.12	1.50	0.19	0.070	0.047	0.020

In Figures 2-3 the predictions of the adjusted model are compared to the experimental data. In these plots the temperatures to 5%, 50% and 95% of the reaction ($T_{5\%}$, $T_{50\%}$ and $T_{95\%}$) are shown as a function of the cooling rate for several steels. It can be seen that the transformation model correctly describes the dependence of the reaction kinetic on the cooling rate, as well as the delaying effect produced by the different alloying additions.

The release heat during the reaction and the specific heat of the system, needed for the coupling to the thermal model, were derived from the free energy using thermodynamic relationships. The free energy of the system composed of austenite, ferrite, perlite and bainite was calculated, as a function of temperature and time, using the rule of mixing proposed in reference [18].

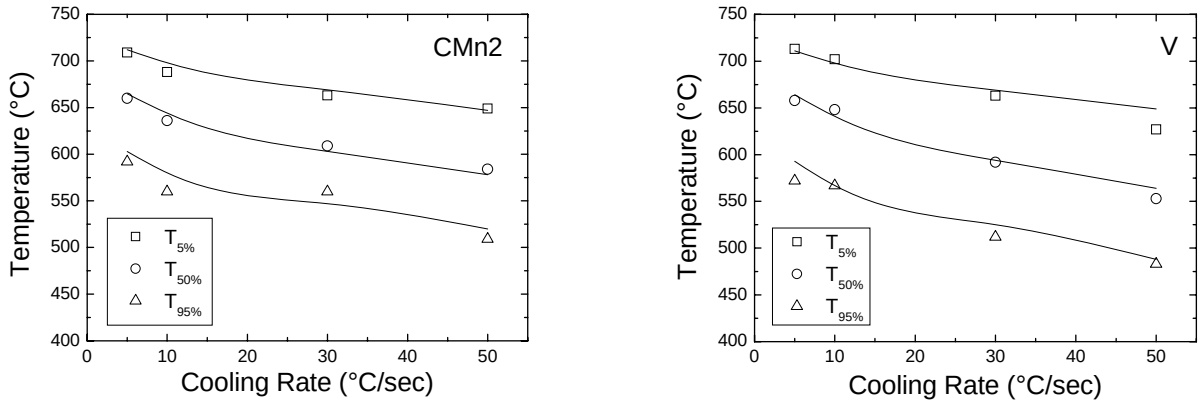

Figure 2: Comparison between experimental values (symbols) and theoretical calculations (lines) of temperatures to 5, 50 and 95% of transformation (T5%, T50% and T95%). Left: CMn2 steel. Right: V steel.

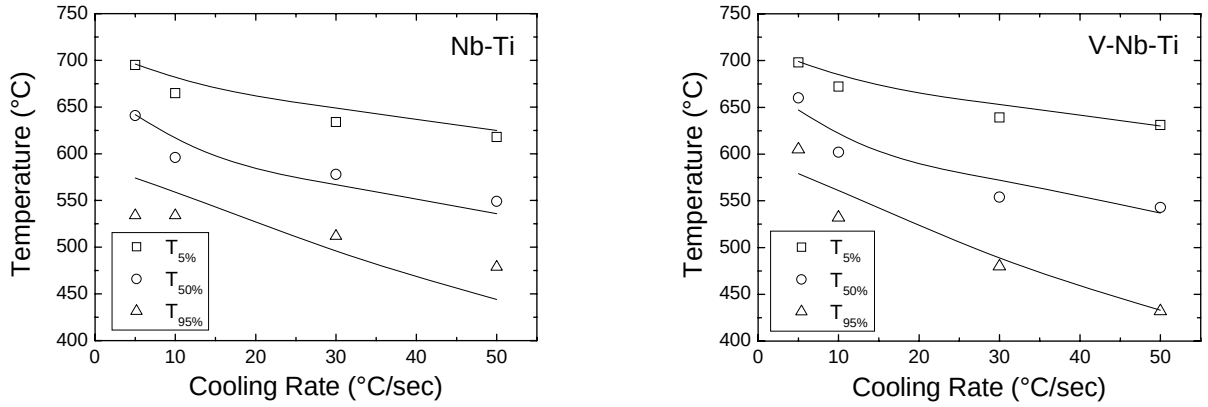

Figure 3: Comparison between experimental values (symbols) and theoretical calculations (lines) of temperatures to 5, 50 and 95% of transformation (T5%, T50% and T95%). Left: Nb-Ti steel. Right: V-Nb-Ti steel.

3. Thermal finite element model

The thermal model and the coupling to the metallurgical model were described in detail in [24]. For an isotropic material the diffusion equation to be solve by the finite element method [25] is

$$\frac{\partial h}{\partial t} - \underline{\nabla}.(k\underline{\nabla}T) = 0 \qquad (5)$$

where h is the enthalpy of the solid solution, k is the thermal conductivity and T the temperature. For each material point, h is function of the temperature and the phase distribution.
The first term of the diffusion equation can be dealt as follows

$$\frac{\partial h}{\partial t} = \left.\frac{\partial h}{\partial T}\right|_{X^\phi} \frac{\partial T}{\partial t} + \left.\frac{\partial h}{\partial X^\phi}\right|_{T} \frac{\partial X^\phi}{\partial t} \qquad (6)$$

where the derivates are calculated by the metallurgical model:

$$\left.\frac{\partial h}{\partial T}\right|_{X^\phi} = Cp = -T\left(\frac{\partial^2 G}{\partial T^2}\right)_P \qquad (7)$$

The derivation of eq. (7) is made on a fixed temperature interval, using the present step temperature and the previous step microstructure. Where *Cp* is the specific heat, *G* is the free energy Gibbs and *P* is the pressure.
The release heat during the reaction per unit time (*L*) is

$$\left.\frac{\partial h}{\partial X^\phi}\right|_{T} \frac{\partial X^\phi}{\partial t} = \frac{\partial h}{\partial t} - Cp\frac{\partial T}{\partial t} = L \qquad (8)$$

Between two time steps (t, $t+\Delta t$) , L is calculated with the following expressions

$$L = \frac{\left({}^{t+\Delta t}h - {}^{t}h\right)\Big|_{t+\Delta t T}}{\Delta t} \qquad h = G - T\left(\frac{\partial G}{\partial T}\right)\Big|_{P} \qquad (9)$$

The derivation of eq. (9) is made on a fixed temperature interval, using the present step temperature. The nonlinearity due to the dependency of the temperature with the properties is solved using a Line Search scheme [26]. The transient heat transfer equation is solved using an implicit Euler Backward time integration method [25].

4. Application of the thermal metallurgical model to the cooling table

A diagram of TerniumSiderar cooling table is shown in Figure 4.

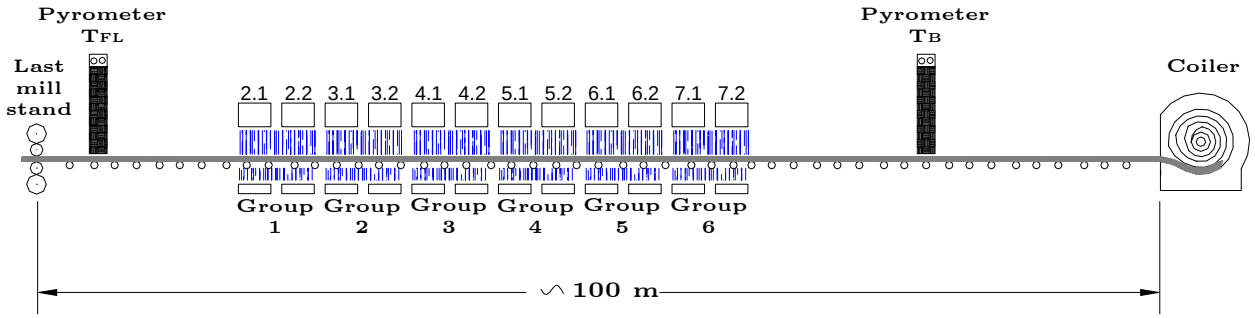

Figure 4 – TerniumSiderar cooling table scheme.

In both the upper and the under side, the strip is cooled by several groups of water jets and the obtained heat transfer coefficient depends on the water impingement

To ascertain the strip temperature along the runout table, pyrometers are placed at the beginning of the cooling table (T_{FL} finish mill temperature) and at the end (T_B coiling temperature).

The necessity to reduce calculation time leads us to use a Lagragean formulation, where a unidimensional section of this strip is modeled. In the strip transverse direction, chemical composition, T_{FL} temperature, water flow rate and austenitic grain size are assumed homogeneous.

The austenitic grain size is predicted by a metallurgical program that models the industrial hot rolling from the overheating furnace to the runout table. The model takes into account the temperature reached in the overheating furnace, the steel chemical composition and the hot rolling sequence [27].

The strip cooling is modeled using three different heat transfer coefficients that take into account different cooling regimes:

- *Dry zones:* places where there is not any water and the cooling is made by convection and radiation with the air. In this case the emithance of the steel is calculated using Seredinski [28] formulation.

$$\varepsilon(T) = 1.1 + \frac{T}{1000}\left[0.125\frac{T}{1000} - 0.38\right] \qquad (10)$$

In order to fit the convection heat transfer coefficient, a trial was performed in TerniumSiderar: a strip was passed through cooling table remaining the water jets closed and measuring T_{FL} and T_B temperatures.

-.*Wet zones*: places where the water jets impinge on the strip surface. The heat transfer coefficient for water cooling surface is modeled using a Hodgson formulation [29, 30] that depends on both strip temperature (Ts) and water flux rate ($\dot{W}$), as shown in equation (11), Figure 5

$$h = A\dot{W}^{B}\left[T_S - n(T_S - T_n)\right]^{C} m \qquad (11)$$

$$m = 1 - \frac{1}{\exp\left[(T_S - T_m)/M\right] + 1}$$

$$n = 1 - \frac{1}{\exp\left[(T_S - T_n)/N\right] + 1}$$

h [kW / m^2 K]

$\dot{W}$ [l / s m^2]

T_S [°C]

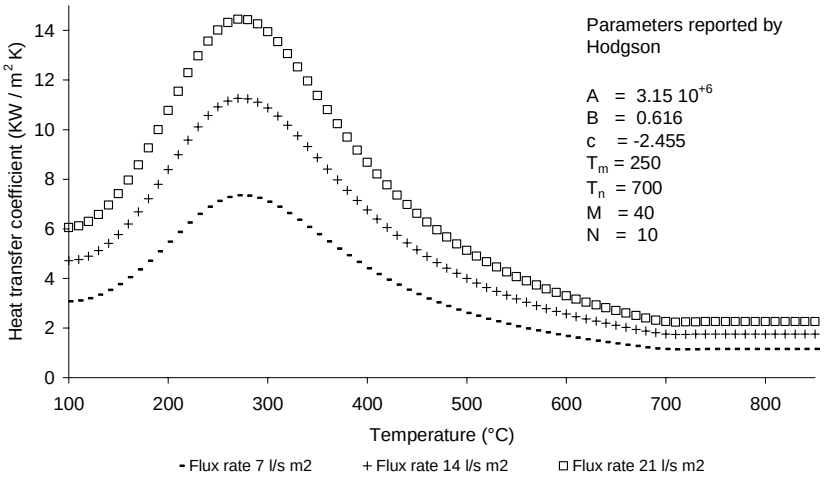

Figure 5 – Heat transfer coefficient for wetting zones

- *Humid zones:* places where residual water creates a stable boiling film. A coefficient presented by Chang [31] that take into account steam physical properties and the temperature surface, is used to model the heat transfer.

Model fitting

For several process conditions, the heat transfer coefficients were fitted by comparing the numerical model predictions and the on-line temperatures measured in the cooling table.
In order to adjust the heat transfer coefficient in the wet zones for the upper side, the empirical parameters A and B were fitted, keeping the rest (C, T_m, T_n, M, N) equal to those reported by Hodgson [29, 30], Figure 5. The under side heat transfer coefficient was adjusted by a proportional constant to the fitted upper side coefficient. The dependency of equation (11) with the $\dot{W}$ was modified to fit a maximum $\dot{W}$ that saturates the heat transfer coefficient for higher water flux rates.
In Figure 6 the predictions of the adjusted model are compared with the on-line T_B temperatures data collected in TerniumSiderar plant, for a C-Mn steel strip and 9.50 mm thickness.

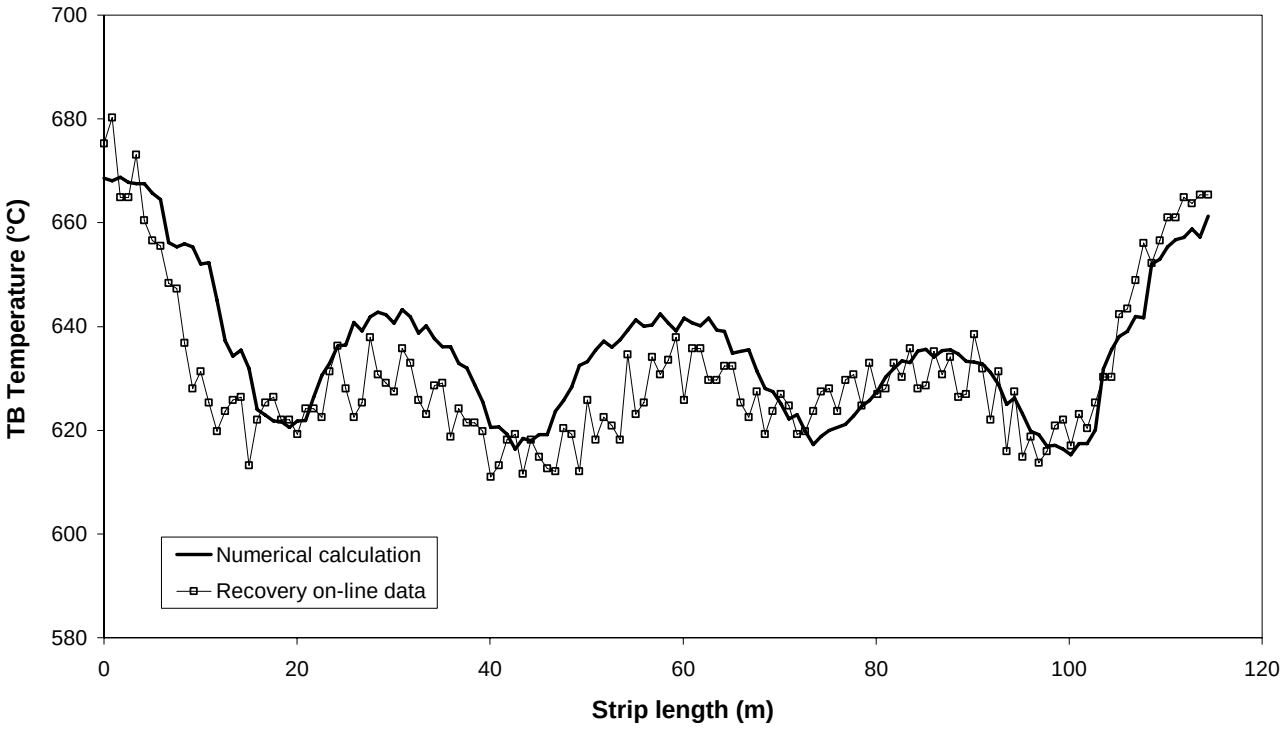

Figure 6 – Comparison between the on-line T_B temperature data and the temperature calculated by the coupling model

5. Model validation

About 300 C-Mn steel coils with different thicknesses (4.75 mm→ 12.70 mm) and process variables were analyzed. Each coil was modeled in approximately 130 sections, which means sampling 40,000 data.
In order to validate the model, an average parameter was established for each coil as follows

$$Error = \left(T_B^{\,numeric} - T_B^{\,measure}\right) \qquad (12)$$

$$Error\% = \left(\frac{\left(T_B^{\,numeric} - T_B^{\,measure}\right)}{T_B^{\,measure}}\right) * 100 \qquad (13)$$

Results in Table II show that very good predictions have been obtained, with less than 5 % errors in 95% of the cases studied.

Table II – Comparison between the on-line T_B temperature and the THERMET results for wide range of thicknesses.

Thickness (mm)	Number of coils	TB temperature average (°C)	Error (°C) [TB_{num} - TB_{meas}]	Error %
4.75	3	610	30	4.9
	3	590	10	1.7
5.00	5	630	20	3.2
5.60	67	620	-10 a -20	-2
6.35	9	600	10	1.7
6.40	9	600	10	1.7
	2	620	5	0.8
	1	610	10	1.6
6.70	4	600	20	3.3
6.90	11	580	0 a 20	2
7.00	4	590	0	0
7.10	14	600	0	0
7.90	4	600	0 a -5	-0.7
8.00	4	610	0 a +5	0.7
	20	630	-10 a -20	-2
	7	640	-50	-7.8
	70	640	-10 a -30	-4
	1	630	-30	-4.7
8.70	11	630	-30	-4.7
	6	630	-60 a -70	-9.5
8.80	15	630	5 a 10	1
9.50	17	630	5	0.8
12.50	3	640	0	0
	3	640	0	0
12.70	12	630	0	0

6. Conclusions

A thermo metallurgical coupling model was developed for TerniumSiderar cooling table. The metallurgical model was adjusted for the range of chemistries and cooling rates of interest. The heat transfer coefficients for the thermal model were fitted using on-line process variables.

Not only the program predicts the T_B temperature accurately but also the T_B temperature shape along the strip and the final microstructure. When the T_B model predictions were compared with plant measurements less- than- 5 % errors were observed in 95% of the cases studied; while it was 10 % in only 13 coils.

7. References

1. N. Hatta, Y. Tanaka, H. Takuda and J. Kokado, ”A numerical study on cooling process of hot steel plates by a water curtain,” *ISIJ International*, 1989, no 8: 673-679.
2. N. Hatta and H. Osakabe, “Numerical modeling for cooling process of a moving hot plate by a laminar water curtain,” *ISIJ International*, 11 (1989), 919-925.
3. M. Raudensky, L. Bending, J. Horsky, “Experimental study of heat transfer in process of rolls cooling in rolling mills by water jets,” *Steel Research*, 1 (1994), 29-35.
4. V.H. Hernandez, I.V. Samarasekera, J.K, Brimacombe, “Heat transfer model of runout table cooling: a fundamental approach” (Paper presented at the 36th Mechanical Working and Steel Processing Conference Proceedings, 1995), 345-356.
5. J.C. Fry, H.D. Morgan, W.D. Morris, J.O. Medwell, “Design of steady state apparatus to evaluate heat transfer coefficient of spray,” *Ironmaking and Steelmaking*, 1 (1997), 1:47-52.
6. H. Robidou, H. Auracher, P. Gardin, M. Lebouché, “Controlled cooling of a hot plate with a water jet,” *Experimental Thermal and Fluid Science*, 26 (2002), 123-129.
7. J.E. Evans, I. D. Roebuck, H.R. Watkins, “Numerical modeling of hot strip mill runout table cooling,” *Iron and Steel engineer*, 1 (1993), 50-55.
8. J. Filipovic, R. Viskanta, F.P. Incropera, “Cooling of a moving steel strip by an array of round jets,” (paper presented at 35th Mechanical Working and Steel Processing Conference Proceedings, 1994), 317-327.
9. T. Kato, Y. Hayasi, T. Kuraishi, S. Ayano, T. Kashimazaki, “New temperature control system of hot strip mill run out table,” (Paper presented at 36th Mechanical Working and Steel Processing Conference Proceedings, 1994), 311-316.
10. M.M. Prieto, L.S. Ruiz and J.A. Menéndez, “Thermal performance of numerical model of hot strip mill runout table,” *Ironmaking and steelmaking*, 6 (2001), 474-480.
11. S.D. Cox, S.J. Hardy, D.J. Parker, “Influence of runout table operation setup on hot strip quality, subject to initial stip condition: heat transfer issues,” *Ironmaking and Steelmaking*, 5 (2001), 363-372.
12. A. Kumar, C. McCulloch, E.B. Hawbolt, I.V. Samarasekera, “Modelling thermal and microestructural evolution on runout table of hot strip mill,” *Materials, Science and Technology*, 7 (1991), 360-367.
13. A. Prasad, S. Jha, N. Mishra, “Modelling of microstructural evolution during accelerated cooling of hot strip on the runout table,” *Steel Research*, 10 (1995), 416-423.
14. A. Prasad, S. Jha, N. Mishra, “Modelling of microstructural evolution during accelerated cooling of hot strip on the runout table,” *Steel Research*, 10 (1995), 416-423.
15. G.R. Gomez, M. Bühler and T. Perez, “Austenite decomposition in low carbon steels with microalloy additions”, (Paper presented at Proceedings of the International Conference on Microalloying for New Steel Processes and Applications, Donostia-San Sebastian, Spain, September 2005), 395.
16. J.W. Christian, *Theory of Transformations in Metals and Alloys*, (2nd ed. Part I, Pergamon Press, Oxford, United kingdom, 1975).
17. J.B. Gilmour, G.R. Purdy and J.S. Kirkaldy: *Metall. Trans*. 3 (1972), 1455.
18. J. Miettinen, “Simple semiempirical model for prediction of austenite decomposition and related heat release during cooling of low alloyed steels,” *Ironmaking and Steelmaking*, 23 (1996), 346.
19. M. Enomoto and H.I. Aaronson, *Metall. Mater. Trans*,.l.17A (1986), 1385.

20. J. Ågren: Scripta, *Metallurgica,* 20 (1986), 1507.
21. T. Tanaka, H.I. Aaronson and M. Enomoto, *Metall. Mater. Trans*,.26 (1995), 547.
22. H.B. Aaron, D. Faistein and G. Kotler, *Journal of Applied Physics*, 41 (1970), 4404.
23. T. Senuma, M. Suehiro and H. Yada, *ISIJ International*, 32 (1992), 423.
24. J. Schicht, "Modelo Termo-Metalúrgico aplicado al enfriamiento de aceros" (Mechanical degree Thesis, Buenos Aires University, 2004).
25. O.C. Zienkiewicz and R.L. Taylor, *The finite element method* (Vol 1, Ed. Butterworth Heinemann, 2000).
26. H. Matthies and G. Strang, "The solution of nonlinear finite element equation," *International Journal for Numerical Methods in Engineering*, 14 (1979), 1613-1626.
27. G. Gomez, T. Pérez and J. Moriconi, "Modelling the Microstructural Evolution during Hot Strip Rolling" (Paper presented at the 44th Mechanical Working and Steel Processing Conference Proceedings, 2002), 1093-1103.
28. F. K. Seredinski, "Prediction of Plate Cooling During Rolling-Mill Operation," *J. Iron Steel Institute*, (1973), 197-203.
29. P.D. Hodgson, K.M. Browne, D.C. Collinson, T.T. Pham and R.K. Gibbs, "A Mathematical Model to Simulate the Thermomechanical Processing of Steel," (Paper presented at Proceedings of 3rd Int. Seminar of the International Federation for Heat Treatment, 1993), 138.
30. P.D. Hodgson, L.O. Hazelden, D.L. Matthews, R.E. Gloss, "The development and application of mathematical models to design thermomecanical processes for long products," (Paper presented at Microalloying conference proceedings, 1995), 341-353.
31. Y.Y. NSU and R.W. Graham, "Transport processes in boiling and two phase system," *American Nuclear society*, (1985).